submitted PRL, 28 May 96.
UM-P--96/41



# THE RAMAN SPECTRUM OF AMORPHOUS DIAMOND

S.Prawer, K.W. Nugent, D.N. Jamieson

School of Physics and Microanalytical Research Centre
University of Melbourne, Parkville, Victoria, Australia, 3052.

## ABSTRACT:

We present the Raman spectrum of an amorphous, fully $sp^3$-bonded carbon network. The reduced Raman spectrum agrees closely with the calculated density of states of diamond. The results have been obtained from nanoclusters produced deep inside a single crystal diamond irradiated with MeV He ions. The deep implantation creates amorphous $sp^3$ bonded C clusters along the ion tracks, within a largely intact diamond matrix. The matrix maintains the clusters under high pressure, preventing the relaxation to $sp^2$ bonded structures. Sharp peaks associated with defect structures unique to MeV ion implantation are observed at 1422, 1447, 1467, 1496, 1540, 1563, 1631, 1649, 1683 and 1726 $cm^{-1}$. We also observe a shoulder in the reduced Raman spectrum at about 1120 $cm^{-1}$ which we tentatively attribute to quantum confinement effects in the carbon nanoclusters. The results provide the Raman signature that might be expected from tetrahedrally bonded amorphous carbon films with no graphite-like amorphous components.

Tetrahedrally bonded amorphous ('diamond-like') carbon has attracted a great deal of both experimental and theoretical interest of the past few years [1]. There have been numerous efforts to model the vibrational spectrum of $sp^3$ bonded amorphous carbon networks, but until now there has been no experimental confirmation, in the form of a Raman spectrum, to test the accuracy of these model calculations. This is primarily because most $sp^3$ rich amorphous carbon films contain a minimum of 5-15% of $sp^2$ bonded carbon. Since the Raman cross-section for $sp^2$ clusters is much greater than that for $sp^3$ bonded structures, scattering from the former dominates the Raman spectrum, producing a broad Raman peak in the vicinity of 1500 $cm^{-1}$, usually swamping the signal from the $sp^3$ bonded portion of the films.

In this paper the Raman spectrum of an amorphous, fully $sp^3$ bonded carbon is reported for the first time, and compared to the calculated density of states of diamond. The measurements are based on a careful examination of the polarized Raman spectrum of diamond implanted with MeV He ions. The MeV ions penetrate deep into the solid creating amorphous clusters along and surrounding the ion track. As these clusters are buried deep inside a largely intact diamond matrix they are maintained under high pressure, and thus do not relax to graphitically-bonded $sp^2$ carbon structures [2,3].

The samples used in the experiments were Type IIa diamond slabs of dimensions 2 x 2 x 0.5 $mm^3$, obtained from the Drukker Corporation (Amsterdam). The main face was oriented along the (100) direction while the edges were oriented along the (010) and (001) directions. All surfaces, including the edges, were polished to a smoothness of about 20 nm. He implantations ($1 \times 10^{17}$ He/$cm^2$, at 3.5 MeV, $R_p \pm \Delta R_p = 7.12 \pm 0.14$ μm [4]) were performed at room temperature into a surface on the edge of sample, as shown in Figure 1. The sample was tilted 7° off axis so as to ensure a "random" orientation for the implantation.

Following the implantations, cross-sectional Raman analysis was performed using a DILOR XY confocal micro-Raman spectrometer and the 514.5nm line from an Ar ion laser. Using a x100 objective, and a confocal aperture of about 100 μm, the volume of the specimen sampled in a typical measurement was a cylinder of diameter 1 μm and height 2 μm. Spectra could then be

collected at one micron intervals from the surface to the end of range [5]. Figure 1 also shows the predicted damage profile for 3.5 MeV ions. In the present work, a region located 1 μm in from the implanted surface was selected for the Raman analysis since in this region the damage density is low, and the diamond structure remains basically intact [4,5].The cross sectional geometry employed (see fig 1) is important because since diamond is transparent, a Raman measurement taken from the implanted surface (as is usually done) will include contributions from many different degrees of damage from the surface extending to and including the end of range. Using the cross-sectional geometry it is possible to ensure that each Raman measurement selectively probes only that level of damage which occurs at the selected depth below the implanted surface. In particular it is possible to exclude any contribution to the Raman spectrum from the end of range damage. At the end of range the nuclear stopping cross section, and hence the damage, reach a maximum, and may exceed the critical value for graphitization of the diamond.

Due to the dipole selection rules, the intensity of the Raman line in diamond is sensitive to the orientation of the diamond with respect to the direction of the polarization vectors of the incident and scattered laser beams [6]. In the present work, a backscattering geometry was employed, with the laser light incident along the [100] direction. With the polarization vector of the incident light parallel to the [010] direction and the analyser polarization set to the [001] direction, the selection rules allow the observation of the first order single phonon diamond line at 1332 $cm^{-1}$ [6]. However, if the polarization vector of the incident beam is parallel to [001] and the analyzer remains fixed parallel to [001], the diamond line is forbidden. Therefore features which are observed in the Raman spectrum both in the allowed and "forbidden" orientations must be due to structures which are not aligned with the cubic symmetery of the diamond lattice such as, for example, local defect structures and amorphous clusters. In the "forbidden" orientation, the diamond line should not be observed at all. However, some polarization leakage does occur to due to the imperfect backscattering geometry in the micro-beam experiment arising from the use of a high numerical aperture objectives to focus the incident laser beam. Using our experimental arrangement, for an undamaged single crystal diamond, the intensity of

the 1332 $cm^{-1}$ diamond line in the "forbidden" orientation is about 8% of that in the allowed orientation, which is the measure of the 'polarization leakage' in the present experiment.

Figure 2 shows the Raman spectrum of the implanted diamond in the allowed and forbidden orientations. In order to take into account the polarization leakage discussed above, the spectrum for the 'forbidden' orientation has been corrected by substracting from it 8% of the allowed spectrum. The spectra have been vertically displaced from one another for clarity but are otherwise displayed on the same vertical scale. As expected, in the allowed spectrum the single phonon diamond line dominates. The shift of this line from its undamaged position at 1332 $cm^{-1}$ and its FWHM have both been shown to vary linearly with increasing defect density [5], and the position of the diamond line in Fig 2 (at 1316 $cm^{-1}$) is consistent with this defect induced shift

In the forbidden spectrum, (Fig 2), the supression of the diamond line allows new features to be observed at a higher signal to noise ratio than would otherwise be possible if the polarization analysis was not carried out. Figure 3 shows the portion of the forbidden spectrum enlarged to display sharp peaks at 1422, 1447, 1467, 1496, 1540, 1563, 1631, 1649, 1683 and 1726 $cm^{-1}$. These peaks are associated with specific defects structures unique to MeV ion implanted diamond and some ( 1451, 1498, and 1634 $cm^{-1}$) have been observed previously [3]. There is some evidence that the peak at 1630$cm^{-1}$ is due to the "dumbell" defect in diamond [7]. When 488nm excitation was used instead of 514.5nm excitation, all the spectral features reported in Figs 2 and 3 were observed at the same wavenumber shift, thus confirming that the observed peaks are due to Raman scattering and not luminesence. A detailed investigation of the dose dependence of the position and FWHM of these peaks and their annealing behaviour will be published elsewhere [8].

A comparison of the allowed and forbidden spectra in figure 2 shows that, except for the diamond line, all other features including the aforementioned sharp Raman peaks and the broad features are reproduced in both spectra. This indicates that the defect clusters are not aligned with the cubic diamond lattice. Note in particular the absence of any broad feature in the region of 1500-1550 $cm^{-1}$ in both the allowed and forbidden spectra. In view of the sensitivity of Raman spectroscopy to $sp^2$ bonded carbon structures, the absence of a broad peak in this region

is convincing evidence that MeV ion implantation does not result in the formation of aromatic or graphite-like $sp^2$ bonded structures, at least in the cap layer away from the end of range damage. For comparison, Figure 3 also shows the Raman spectrum of an amorphous carbon film synthesized by ion beam deposition of 120 eV C ions. The $sp^2/(sp^3+sp^2)$ ratio was determined independently by electron energy loss spectroscopy to be 10-15%. Despite the relatively low $sp^2$ concentration the spectrum in this case is completely dominated by the peak centered around 1550 $cm^{-1}$.

In figure 4, the data for the forbidden orientation are replotted as a reduced Raman spectrum and and are compared to the calculated density of states of diamond . The reduced Raman spectrum is given by

$$I_R(\omega) = I(\omega)/\{[1+n(\omega,T)]/\omega\}$$

where $\omega$ is the frequency of the Raman shift, $I(\omega)$ is the measured inensity of the Raman spectrum and $n(\omega,T) = [\exp(h\omega/kT) - 1]^{-1}$ is the Bose-Einstein distribution. It has been shown that this reduced Raman spectrum should replicate the vibrational density of states [9]. Indeed there is a close match between the DOS of Ge and and Si with their respective reduced Raman spectra [10,11].

Wang and Ho [12] used a tight binding molecular dynamics simulation to study the vibrational properties of diamond-like (ie $sp^3$-bonded) amorphous carbon. In Figure 4, the results of their calculation for the vibrational density of states (DOS) of crystalline diamond has been plotted in order to facilitate a comparison between the calculated and measured DOS. Note that the result extracted from Wang and Ho (Fig 4(b)) is the predicted DOS of states of a diamond lattice, **not** of a disordered amorphous network. Two features are immediately obvious: (i) the spectrum is dominated by a large peak at about 1200 $cm^{-1}$ and (ii) there are no vibrational modes for $sp^3$ bonded carbons at energies exceeding 1400 $cm^{-1}$. These features are reproduced in the results of calculations reported by other authors [13].

Considering the fact that the calculation is for the DOS of crystalline diamond, the match between the calculated and measured DOS is impressive. The major difference appears to be that the measured 1200 $cm^{-1}$ peak is broader than that predicted by the calculation. However, in practice, an amorphous, fully $sp^3$ bonded network would be subject to strain and bond angle disorder and these factors will tend to cause a broadening of the DOS as compared to the single crystal case. The close match between the calculated and measured DOS leads us to conclude that the measured spectrum in Figure 4 is representative of the DOS of 'amorphous diamond', ie clusters of carbon displaying short-range $sp^3$ ordering without any long range order.

One other interesting feature of the measured spectrum is the shoulder present at about 1120 $cm^{-1}$. Such shoulders in the Raman spectrum are often observed in nanocrystalline diamond films synthesized by chemical vapour deposition (CVD). However, the calculated DOS does not show any hint of a feature in this region of the spectrum. One possible explanation is to note that in the case of MeV implanted diamond, the damaged clusters are of the order of 1-2 nm in diameter [14]. Additional modes, due to quantum confinment within these spatially confined regions, could then be observed that would not be predicted by a DOS calculation for crystalline diamond. The results of Fig 4 suggest that the peak at 1120 $cm^{-1}$ may correspond to one of these modes, and implies that CVD films displaying this mode may contain clusters of $sp^3$ bonded material of similar spatial extent to that produced by MeV implantation.

In summary we have obtained the Raman spectrum of amophous $sp^3$ bonded clusters from the Raman spectrum of MeV implanted diamond. The spectrum closely follows the density of states of diamond, with the exception of a shoulder at about 1120 $cm^{-1}$ which we tentatively attribute to modes arising from the small (1-2nm) cluster size. There is still much discussion amongst those attempting to create tetrahedral amorphous carbon by ion beam and other methods whether, in principle, it is possible to produce a completely free of $sp^2$ bonded material. We suggest that the Raman spectrum reported here can serve as a signature for such completely $sp^3$ bonded amorphous carbon networks.

We are very grateful for discussions with Professors Peter Koidl and Rafi Kalish who offered many valuable insights into the present results.

## REFERENCES

[1] See for example, J. Robertson, Prog. Solid State Chem. **21,** 199, (1991).

[2] S. Prawer, D.N. Jamieson and R. Kalish, Phys. Rev. Lett., **69,** 2991, (1992)

[3] J.D. Hunn, S.P. Withrow, C.W. White, D.M. Hembree Jr., Phys. Rev. **B52,** 8106, (1995).

[4] J.F. Ziegler, J.P Biersack and U. Littmark, The Stopping and Range of Ions in Solids, (Pergamon, New York, 1985)

[5] D. N. Jamieson, S.Prawer, K.W. Nugent, and S.P. Dooley, Nucl. Inst. Meth. Phys. Res., **B106,** 641, (1995)

[6]. S. Prawer, S., K.W. Nugent, and P.S. Weiser, Applied Physics Letters **65**: 2248-2250 (1994).

[7] S.Prawer, Mat. Res. Soc. Symp A., Boston 1996, (unpublished)

[8] S. Prawer, K.W. Nugent, D.N. Jamieson, to be published.

[9] R. Shuker and R. Gammon, Phys. Rev. Lett., **25,** 222, (1970)

[10] N. Maley and J.S. Lannin, Phys. Rev **B35,** 2456, (1987)

[11] F. Li and J.S. Lannin, Phys. Rev. **B39,** 6220, (1989)

[12] C.Z. Wang and K.M Ho, Phys. Rev. Lett., **71,** 1184, (1993)

[13] P.J. Lin-Chung, Phys. Rev. **B50,** 16905, (1994)

[14] S. Prawer and R. Kalish, Phys. Rev. **B51,** 15711, (1995).

## FIGURES

**Figure 1.** Schematic showing the geometry used for the implantation and the cross-sectional Raman analysis. The implantation surface is labelled A whilst the analysis surface is labelled B. The heavily damaged region at the end of range of the He ions is shown as a hatched strip. Note that the diagram is not to scale. The dimensions of the implanted area on face A are about 100 x 100 $\mu m^2$. The hatched strip is located about 7 $\mu m$ below the implanted surface. Also shown is the damage profile as predicted by the monte-carlo computer code TRIM [ 4].

**Figure 2:** The measured Raman spectrum of diamond implanted with 3.5 MeV He to a dose of 1 x$10^{17}$ He/$cm^2$ at room temperature. (a) The spectrum for the diamond in an orientation in which the dipole selection rules allow the triply degenerate diamond phonon line to be observed are shown and (b) the spectrum for the orientation in which the selection rules forbid the observation of this mode. The spectrum in the forbidden orientation has been corrected to take into account breakthrough of the diamond line due to polarization leakage (see text).

**Figure 3:** The region of the forbidden spectrum of Fig 2 above 1400 $cm^{-1}$ shown in more detail. Peask are observed at 1422, 1447, 1467, 1496, 1540, 1563, 1631, 1649, 1683, and 1726 $cm^{-1}$. Note the absence of any broad features in the region of 1500-1550 $cm^{-1}$ which are characteristic of aromatic or graphite-like $sp^2$ bonded carbon structures. For comparison, the Raman spectrum from an amorphous carbon film containing more than 85% $sp^3$ bonding is shown.

**Figure 4**: The reduced Raman spectrum of MeV implanted diamond (in the forbidden orientation) shown in more detail. The calculated DOS of crystalline diamond taken from the work of Wang and Ho [12] is shown for comparison.

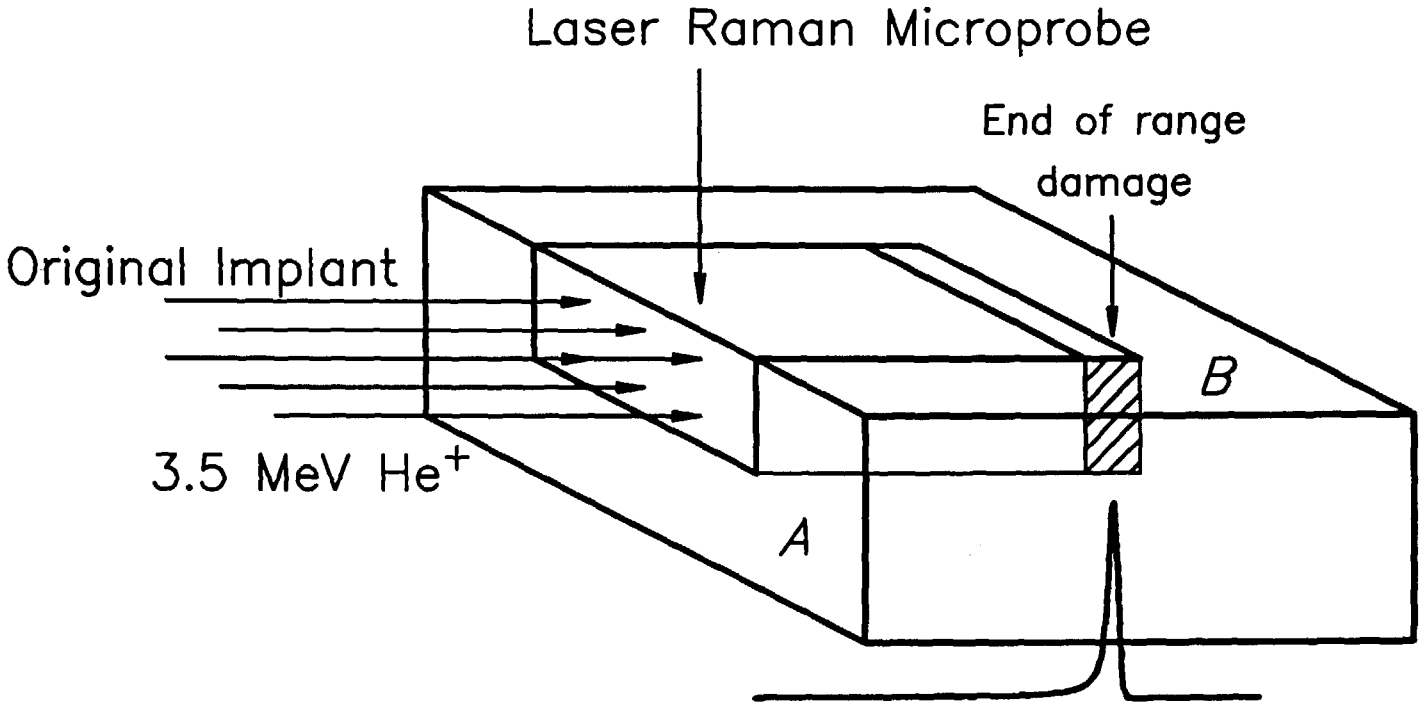
Laser Raman Microprobe
End of range
damage
Original Implant
3.5 MeV $He^+$
B
A

Fig 1

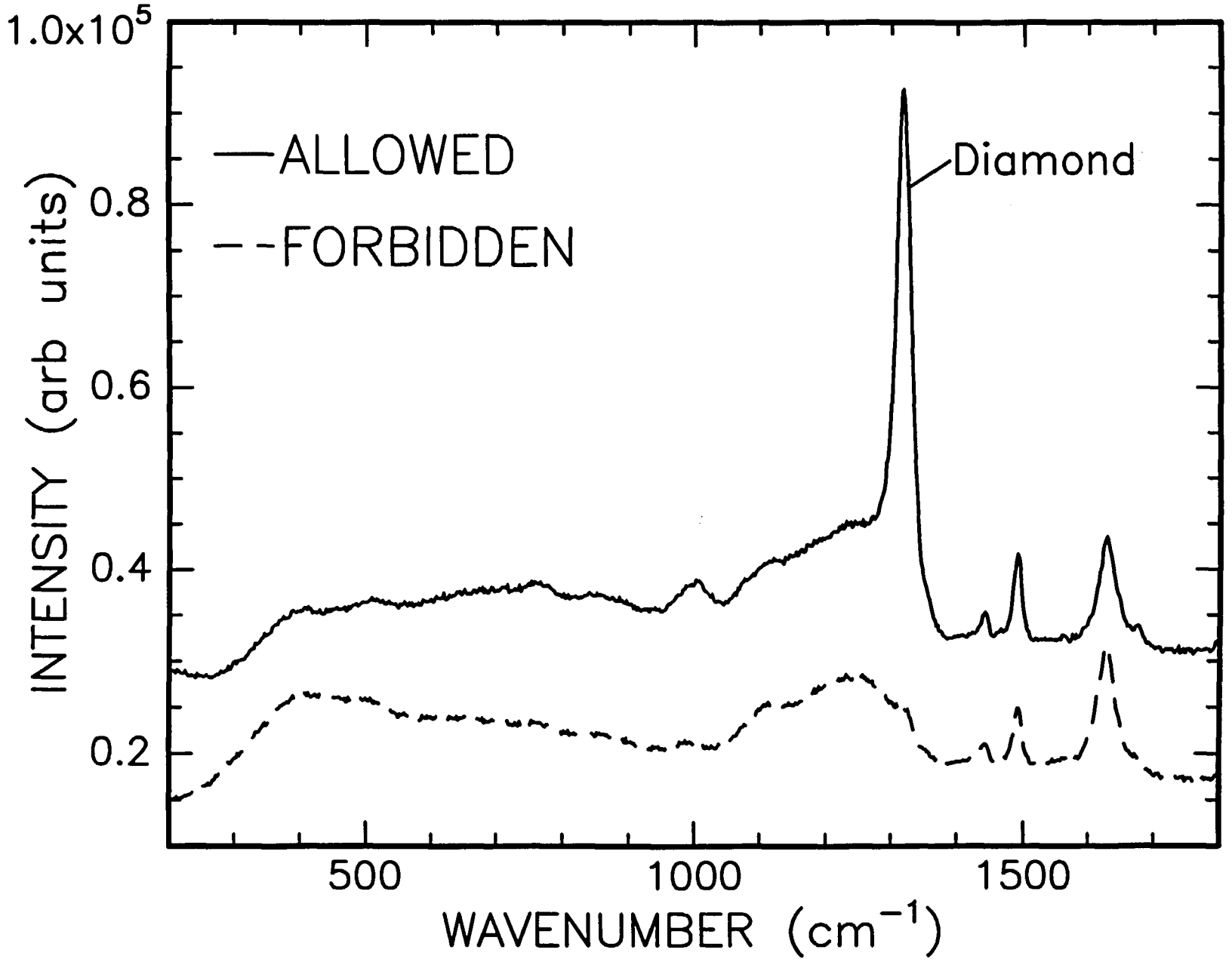
1.0x10^5
0.8
0.6
0.4
0.2
INTENSITY (arb units)
—ALLOWED
--FORBIDDEN
Diamond
500
1000
1500
WAVENUMBER (cm^-1)

Fig 2.

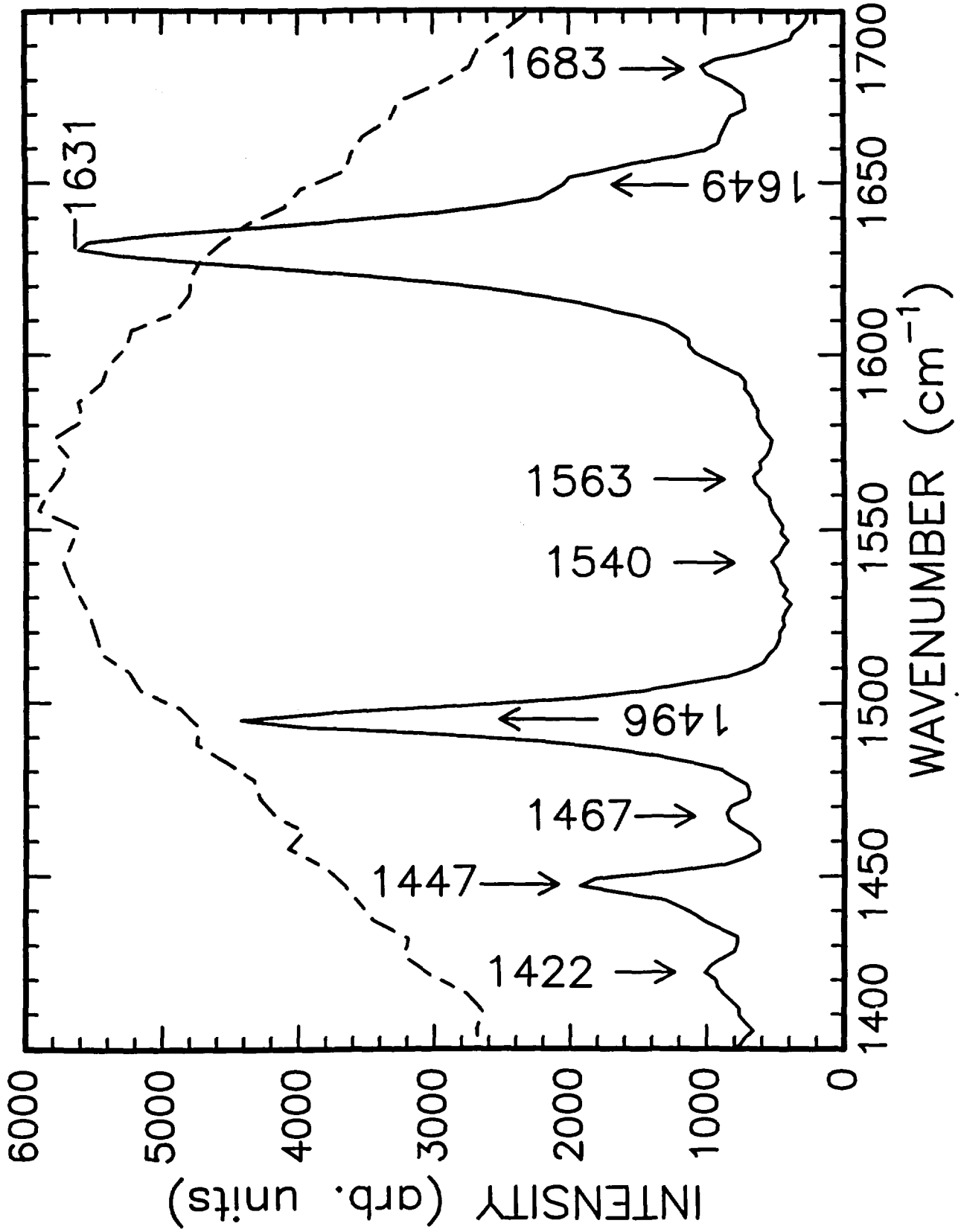
1683
1649
1631
1563
1540
1496
1467
1447
1422
1400
1450
1500
1550
1600
1650
1700
WAVENUMBER (cm⁻¹)
0
1000
2000
3000
4000
5000
6000
INTENSITY (arb. units)

Fig 3

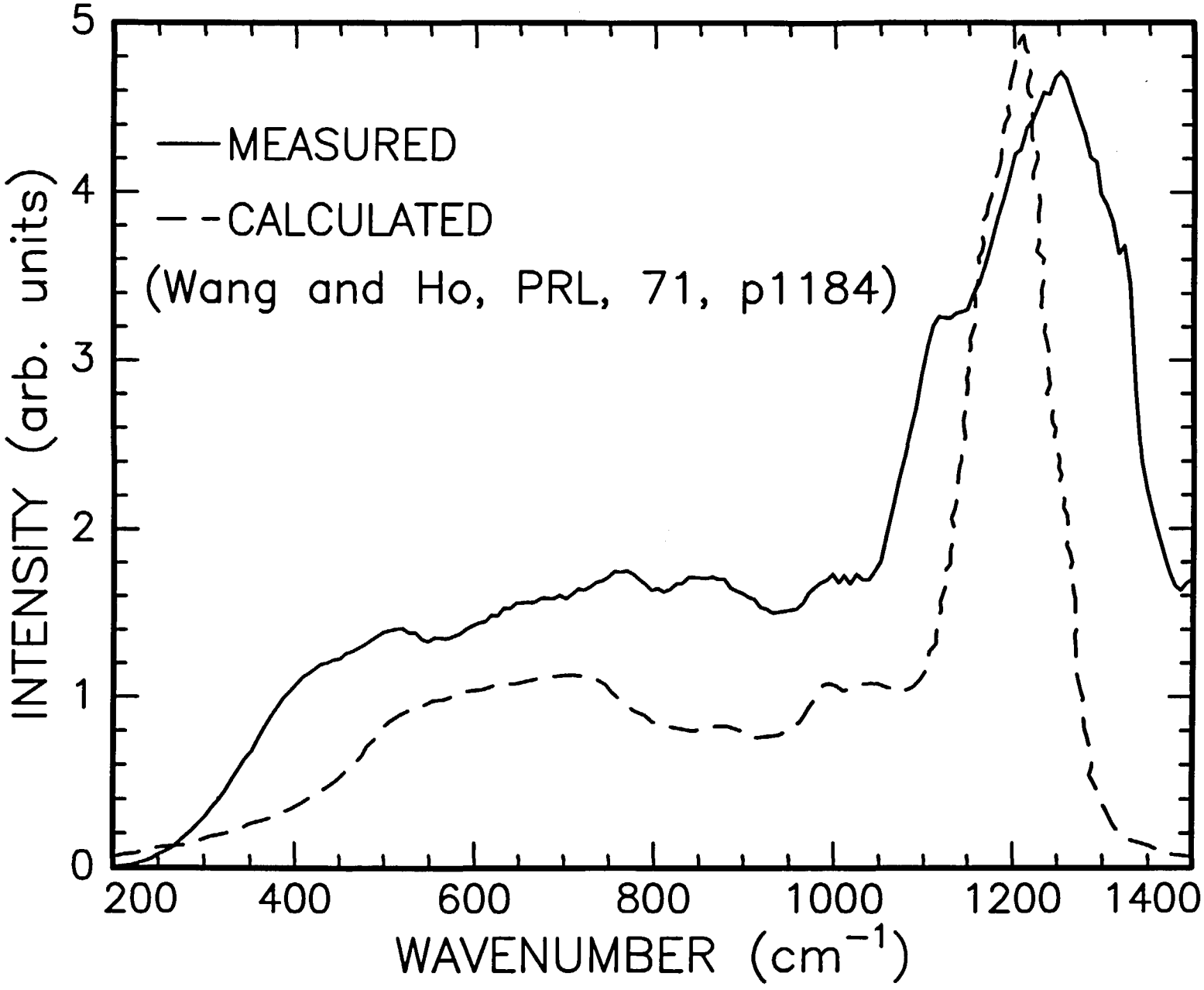
MEASURED
CALCULATED
(Wang and Ho, PRL, 71, p1184)
INTENSITY (arb. units)
WAVENUMBER (cm$^{-1}$)
0
1
2
3
4
5
200
400
600
800
1000
1200
1400

Fig 4